第51卷第4期 光 子 学 报 Vol.51 No.4
2022年4月 ACTA PHOTONICA SINICA April 2022

引用格式：LONG Jun, CAI Ping, PAN Shuyuan, et al. Phase Stitching Based Multi-CCDs Deformation Measurement in Digital Speckle Pattern Interferom[J]. Acta Photonica Sinica, 2022, 51(4):0412003
隆军,蔡萍,潘淑媛,等.数字散斑干涉形变测量中基于多CCD的相位拼接[J].光子学报,2022,51(4):0412003

数字散斑干涉形变测量中基于多CCD的相位拼接

隆军[1,2],蔡萍[1,2],潘淑媛[1,2],刘持越[1,2],闫浩[1,2]
(1 上海交通大学 电子信息与电气工程学院,上海 200240)
(2 上海智能诊疗仪器工程技术研究中心,上海 200240)

摘　要: 在数字散斑干涉测量中,对于给定尺寸的CCD,很难在不影响形变测量横向分辨率的情况下扩大视野。针对该问题,提出了一种在不影响横向分辨率的情况下拼接多个子图像相位以扩大视野的方法。设计并搭建了一套多CCD实验装置来获取多个子图像。利用重叠区域解包裹后的相位图估计相邻子图像之间的相对位置并补偿相位偏差,实现正确的相位拼接。为了使用尽可能少的CCD获得尽可能大的视野,分析了重叠区域大小对拼接效果的影响。权衡视野和精度,重叠区域的最佳尺寸约为10%。所提方法在只使用两个CCD的条件下实现了视野从5.5 cm×4 cm扩大到10 cm×4 cm。拼接前后重叠区域的最大相对误差小于1%,证明了该方法的有效性。此外,还比较了所提方法与单CCD的形变测量均方根误差(RMSE)。结果表明,提出的方法具有与单CCD形变测量接近的测量精度。

关键词: 数字散斑干涉;相位拼接;相位偏差;形变测量;多CCD
中图分类号: O438.1　　**文献标识码:** A　　**doi:** 10.3788/gzxb20225104.0412003

0 Introduction

Digital Speckle Pattern Interferometry (DSPI) [1-2] provides an effective means of full-field and non-contact measurement of deformation or displacement. It has been widely used in material properties analysis[3-7], structural design verification[8], and thermal stress analysis[9]. With the advancement of the aerospace and automotive industry, deformation measurements with a large Field of View (FOV), high resolution and wide measurement range are becoming more and more urgent. The synthesis of multiple sub-holograms has proven effective in increasing the field of view and improving the lateral resolution of Digital Holography (DH)[10-12].

In the current DH aperture synthesis methods, sub-holograms are obtained by a multi-step image acquisition operation as the object or camera is scanned along the x and y-axis[10,12-15]. In the case where there is a certain overlap area between adjacent sub-holograms, the aperture synthesis algorithm can stitch all the sub-holograms by image registration to obtain a full-field hologram. This method assumes that two neighboring sub-holograms have the same intensity distribution in the overlapping region. It is only applicable to the measurement and observation of stationary objects. In DH or DSPI deformation measurements, two surface states of the object are involved, corresponding to before and after deformation, and the full-field deformation is obtained by subtracting the pre-deformation hologram or interferogram note from the post-deformation hologram or interferogram. Positioning errors in objects or cameras during successive sub-image acquisitions can lead to mismatches in the position of the corresponding pixels of the stitched image before and after the

Foundation item: National Key Research and Development Program of China (No. 2016YFF0200700)
First author: LONG Jun (1987—), male, Ph.D. candidate, mainly focuses on digital speckle pattern interferometry and digital holography. Email: water19111213@sjtu.edu.cn
Supervisor (Contact author): CAI Ping (1963—), female, professor, Ph. D. degree, mainly focuses on digital speckle pattern interferometry and digital holography. Email: pcai@sjtu.edu.cn
Received: Sep.18, 2021; **Accepted:** Nov.11, 2021

deformation, which may invalidate the resolved deformation. In addition, axial misalignment between corresponding hologram pairs will result in stitching failure[14,16].

The use of multiple CCDs to cover the full field of view can overcome the disadvantages of multi-step image acquisition schemes. However, the relative positions among the CCDs need to be addressed. Using multi-CCDs to cover the full field of view can overcome the drawback of the multi-step image acquisition scheme. However, the relative positions among CCDs need to be addressed. This is usually estimated by calculating the similarity of intensity images in overlapping regions between adjacent images[13-14,17-18]. However, the intensity distribution in the overlapping areas is usually unequal due to non-uniform illumination light, angular differences between the reference and object beams and differences in the CCD, which affects the correctness of the relative position estimation. Therefore, a method is proposed to estimate relative positions based on the consistency of unwrapped phase maps between adjacent CCDs. At the same time, phase deviations between sub-images of multiple CCDs in the overlapping area caused by the distinct phase reference points of sub-images can be compensated for. Additionally, multi-CCDs solutions pose the problem of bulky and uneconomical systems, so the size of the overlap region should be as small as possible.

To evaluate the effectiveness of image registration of multi-CCDs DSPI system, a dual-CCDs DSPI system was constructed, the relative positions between CCDs were estimated based on the unwrapped phase diagram, the effect of the size of the overlapping area on the image registration accuracy was analyzed, and a compensation method of the phase deviation between CCDs was proposed. Finally, the registration accuracy of the stitching method is evaluated with a calibrated artifact.

1 Method

The optical setup of the two CCD DSPI system is shown in Fig. 1. The light source is a laser with a wavelength of 532 nm. A fiber optic coupler and beam splitter are used to split the laser beam into two beams, one of which serves as thereference light while the other is the illumination light, forming α, β angle with the optical axis of the CCDs ($\beta = 45^\circ$ in our setup). The backscattered light from the object is collected by a lens with a focal length of 85 mm, which is approximately 96 mm from the CCD sensor. There is an aperture in front of the lens to reduce high high-frequency noise and to limit the size of the first-order spectrum in the Fourier transform domain. The reference and object beams are brought together by a 50:50 beam combiner in front of the CCD sensor. Each CCD records the corresponding sub-speckle pattern and transmits it to the computer for sequential data processing. To improve the quality of the interferogram, an NDF is used to adjust the intensity ratio between the object beam and the reference beam. Note that the distance between NDF and the outlet of optical fiber should be as small as possible to avoid the influence of the NDF on the wavefront of reference wavefront.

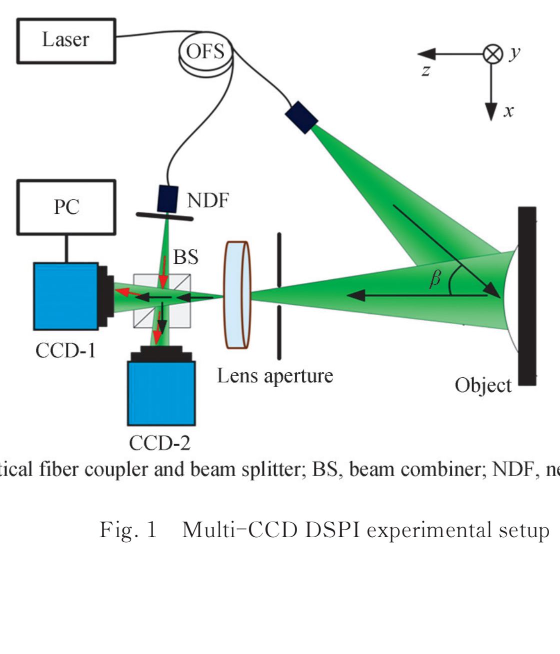

OFS, optical fiber coupler and beam splitter; BS, beam combiner; NDF, neutral density filter

Fig. 1 Multi-CCD DSPI experimental setup

The speckle interferograms before $I_b(x,y)$ and after $I_a(x,y)$ the object surface deformation are recorded with each CCD, one of the interferograms obtained by CCD#1 and CCD#2 are shown in Fig.2 (a) and (b), respectively. By using the Fourier-transform method[19], the phase difference $\delta(x,y)$ caused by the deformation or displacement of the object surface is obtained. After noise suppression filtering[20] and phase unwrapping[21], the unwrapped phase maps ($\varphi_p(x,y)$ and $\varphi_q(x,y)$) of each CCD are obtained. The flow chart of proposed method of phase stitching is shown in Fig. 2.

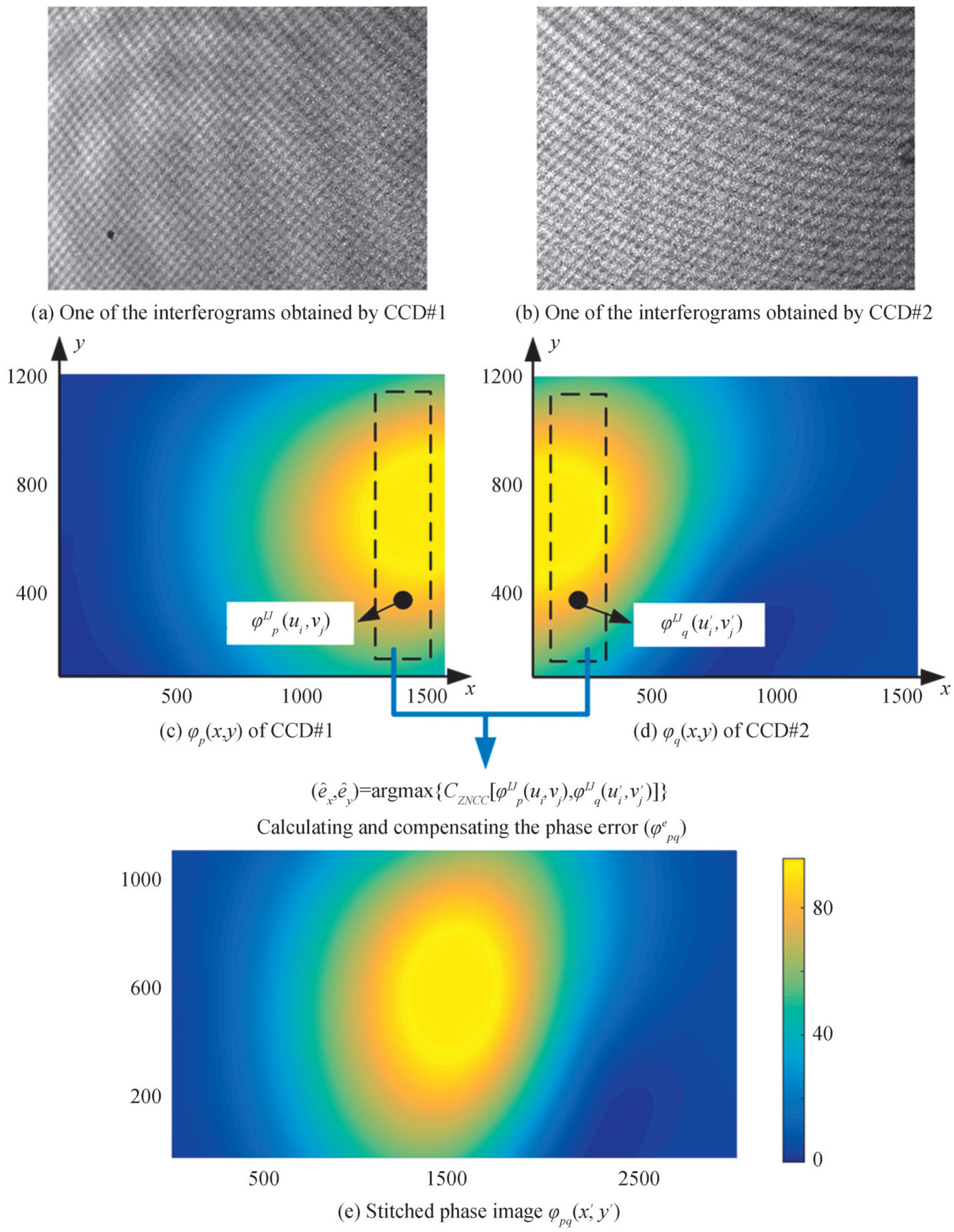

Fig. 2 The flow chart of proposed method of phase stitching

After the unwrapped phase maps are obtained, shown as Fig. 2(c) and (d), assuming a set of relative positions (e_x, e_y), calculating the similarity between the phase $\varphi_p^{IJ}(u_i, v_j)$ and $\varphi_q^{IJ}(u'_i, v'_j)$ of the overlapping area by Zero-Normalized Cross-Correlation (ZNCC) criterion[22].

$$C_{\text{ZNCC}}(e_x, e_y)=\sum_{i=1}^{I}\sum_{j=1}^{J}\left[\frac{\varphi_p^{IJ}(u_i,v_j)-\varphi_p^m}{\sum_{i=1}^{I}\sum_{j=1}^{J}[\varphi_p^{IJ}(u_i,v_j)-\varphi_p^m]^2}\times\frac{\varphi_q^{IJ}(u'_i,v'_j)-\varphi_q^m}{\sum_{i=1}^{I}\sum_{j=1}^{J}[\varphi_q^{IJ}(u'_i,v'_j)-\varphi_q^m]^2}\right] \tag{1}$$

where the overlapping area of the two unwrapped phases is $I\times J$ pixels, $u'_i=u_i-e_x, v'_j=v_j-e_y$

($i\in[1,I]$, $j\in[1,J]$) $\varphi_p^U(u_i,v_j)$ and $\varphi_q^U(u'_i,v'_j)$ denote the phase value at coordinates (u_i,v_j) and (u'_i,v'_j) of the overlapping area of the CCD#1 and the CCD#2, respectively; and φ_p^m and φ_q^m are the mean values of the overlapping area of the CCD#1 and the CCD#2, respectively.

The ZNCC criterion defined in Eq. (1) is a parametric objective function involving two unknown parameters of the relative positions (e_x,e_y) of the two CCDs. Mathematically, this becomes a parametric optimization problem. The position corresponding to the maximum value of the objective function Eq. (1) is the best estimate of the relative position $(\hat{e}_x,\hat{e}_y)$. Then the phase error (φ_{pq}^e) between $\varphi_p^U(u_i,v_j)$, in the overlapping area can be calculated by Eq. (2). Note that the relative position $(\hat{e}_x,\hat{e}_y)$ between CCDs needs to be solved once, but the phase error (φ_{pq}^e) under different deformation values needs to be solved every time.

$$\varphi_{pq}^e=\frac{1}{I\times J}\left[\sum_{i=1}^{I}\sum_{j=1}^{J}\varphi_p^U(u_i,v_j)-\varphi_q^U(u'_i,v'_j)\right] \tag{2}$$

Then compensating the phase deviation between CCDs by Eq. (3) and

$$\varphi'_q(x,y)=\varphi_q(x,y)+\varphi_{pq}^e \tag{3}$$

where $\varphi'_q(x,y)$ is the compensated phase map of $\varphi_q(x,y)$. Then a larger unwrapped phase map $\varphi_{pq}(x',y')$ ($x'\in[1,M+e_x]$, $\in[1,N-e_y]$) can be correctly stitched, shown as Fig.2 (e), and the deformation $l_w(x',y')$ can be calculated by Eq. (4).

$$l_w(x',y')=\frac{\lambda}{2\pi}\times\frac{\varphi_{pq}(x',y')}{(1+\cos\beta)} \tag{4}$$

where $l_w(x',y')$ is the out of plane deformation of the tested specimen, λ is the wavelength of the laser, β is the included angle between illumination direction and detection direction.

2 Experiment and results

The experiment setup is shown in Fig. 3, where two CCDs with a pixel size of 4.4 μm ×4.4 μm and 1 600×1 200 pixels were utilized to record multiple sub-images. An artifact fixed to a calibrated loading device was employed to investigate the proposed method. The deformation is imposed by piezo actuators. The artifact is a disk shape. The displacement of the central area is calibrated with a universal length meter (HELIO-SIP550M). It is often the case that one always expects the maximum field of view from as few CCDs as possible. Therefore, it is essential to explore the effect of overlap area size on the stitching results. Comparing the standard deviation of the difference in overlap area measurements before and after stitching different sizes of overlap areas, the results are shown in Fig. 4. The standard deviation is not sensitive to the size of the overlapping area, the smallest overlap area size in our experiments is 59 pixels and the largest size is 817 pixels

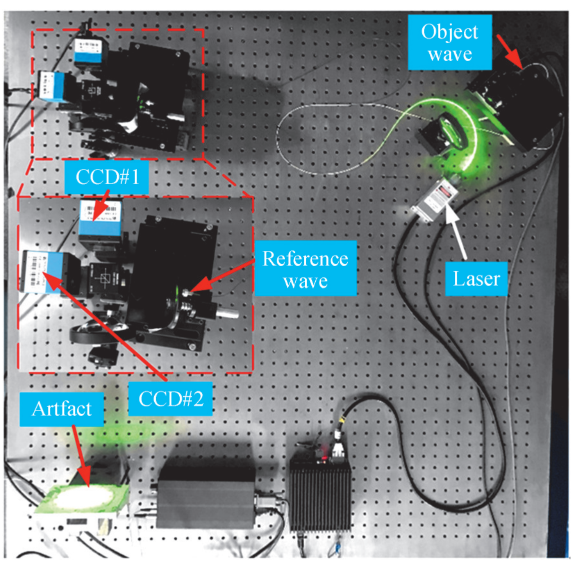

Fig.3 Experiment setup

in the x-axis direction. The maximum standard deviation is less than 0.018 μm and the minimum standard deviation is greater than 0.013 μm, and the difference between them is less than 0.005 μm which is neglibible. The standard deviation is less than 0.015 μm when the size of the overlap area is between 141 and 461 pixels, corresponding to a percentage of the overlap area between 8.8% and 28.8%. Therefore, when using multiple CCDs for phase stitching in the DSPI, it is appropriate to take an overlap area of around 10%.

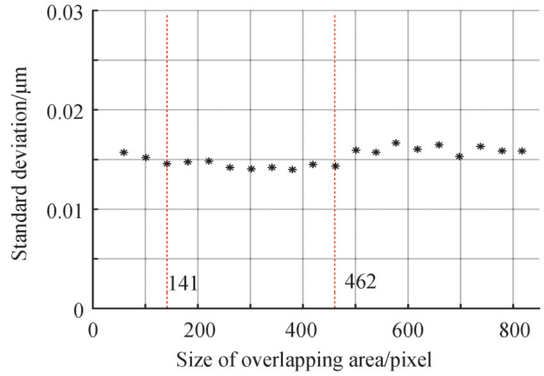

Fig.4 The relationship between the standard deviation of the difference of before and after stitching and size of overlapping area

In order to prove the effective of the proposed method, the relative error which is defined as

$$E(\varphi)=\frac{|\varphi_o-\varphi|}{|\varphi|}\times 100\% \tag{5}$$

where φ_o and φ are the phases of the overlapping region before and after stitching, respectively. When the deformation of the workpiece is 9 μm the unwrapped phase and the relative error of the overlapping region before and after stitching are shown in Fig.5. The FOV expends from 5.5 cm×4 cm to 10 cm×4 cm after stitching. The maximum relative error before and after stitching is less than 1%, which illustrates the effectiveness of the proposed method.

To further evaluate the proposed method, a total of 9 displacement loading points are included, and three groups of values are measured by CCD#1, CCD#2, and the phase stitching method. The fitted curves and residual errors are shown in Fig.6. The Root Means Squared Errors (RMSE) and coefficient of determination R are shown in Table 1. A good fit to a range of discrete deformation values using the Least Square(LS) method is shown in Fig.6(a) and is evaluated quantitatively using the metric R in Table 1. The measurement errors and fitting residuals are shown in Fig. 6(b) are small and illustrate the validity of the measurement method. By comparing the RMES values shown in Table 1, the measurements of the proposed method are more accurate than those of a single CCD. It seems to violate that the errors in stitching must be larger than the measurement of a single CCD. However, it should be noted that the values of the overlapping areas are averaged out during the stitching process, which may account for the lower mean square error of the sutures compared to the single CCD measurements. Maybe the random noise was suppressed during the averaging process.

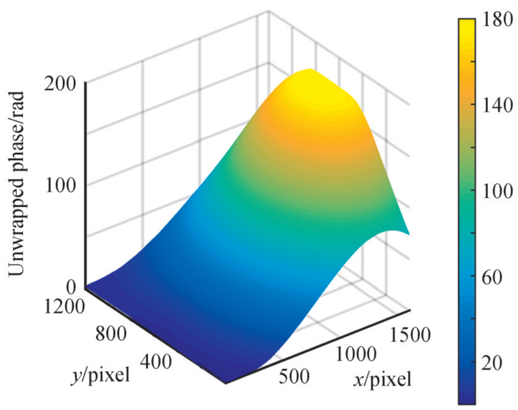

(a) Sub-aperture unwrapped phase map obtained by CCD#1

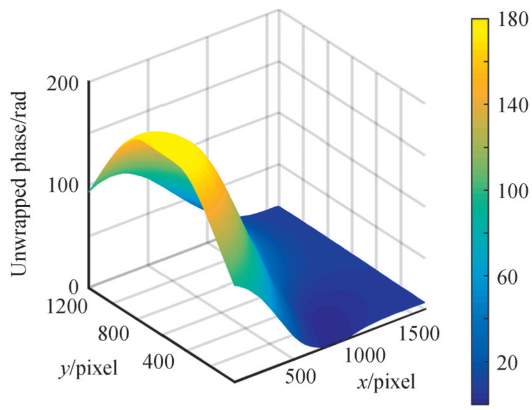

(b) Sub-aperture unwrapped phase map obtained by CCD#2

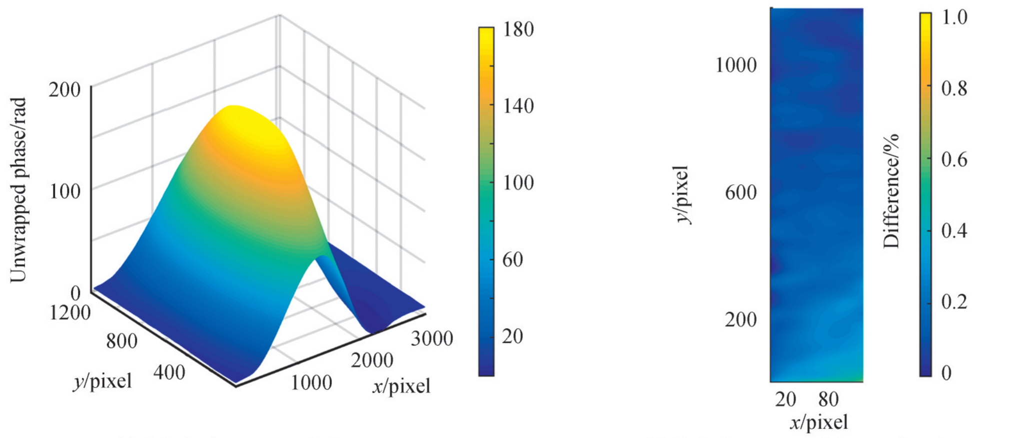

(c) Stitched unwrapped phase map (d) Relative errors of the overlapping area

Fig. 5 Unwrapped phase map and the relative errors of the overlapping area before and after stitching

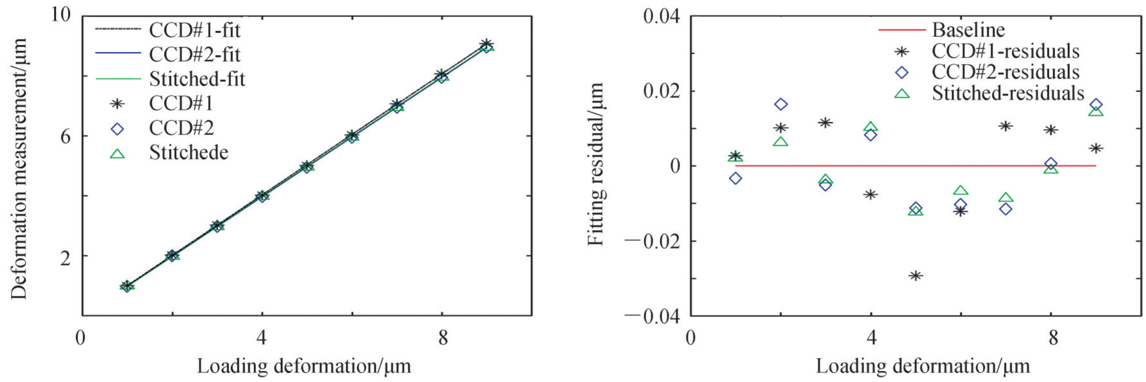

(a) The fitting lines of each group data and corresponding data points (b) The residuals of the fitting

Fig. 6 Least square fitting and fitting residuals

Table 1 The RMSE and *R* of the measurement results

Measuring method	CCD#1	CCD#2	Stitched
R	1.000 0	1.000 0	1.000 0
RMSE /μm	0.015	0.012	0.010

Based on the results obtained above, it can be concluded that phase stitching is effective and allows for FOV expansion.

3 Conclusion

A DSPI system with two CCDs is used to record multiple sub-aperture images to avoid scanning errors in the micro-positioning stage when moving the CCD or object. The registration positions were calibrated to eliminate phase errors between SASPIs. In order to obtain the maximum FOV with fewer CCDs, the relationship between the standard deviation and the size of the overlapping area was investigated. The size of the overlap zone is approximately 10%, which may be appropriate in terms of the trade-off between FOV and accuracy. To demonstrate the effectiveness of the phase stitching method, a calibrated loading device driven by a piezoelectric actuator was used. The measurement accuracy of the phase stitching method is approximate to that of the single-camera method when comparing the measurements of the calibration points by RMSE metric. Since the true value of the full field is unknown, the difference in overlap area between the single CCD method and the phase stitching method was calculated to evaluate the confidence of the full field values obtained by the proposed method, and these values are less than 1%. Furthermore, with more CCDs, the measurement range and axial resolution are increased to a certain FOV.

References

[1] DONG Hui, ZHOU Yan, ZHANG Wanyi, et al. Digital speckle pattern interferometry for deformation measurement[J]. Acta Photonica Sinica, 2010, 39(s1): 19-22.

[2] WU Sijin, YANG Jing, PAN Siyang, et al. Dynamic deformation measurement of discontinuous surfaces using digital speckle pattern interferometry and spatiotemporal three-dimensional phase unwrapping[J]. Acta Photonica Sinica, 2018, 47(2): 0212002.

[3] MA Y H, TAO N, DAI M L, et al. Investigation on vibration response of aluminum foam beams using speckle interferometry [J]. Experimental Techniques, 2018, 42(1): 69-77.

[4] YAN Hao, LONG Jun, LIU Chiyue, et al. Review of the development and application of deformation measurement based on digital holography and digital speckle interferometry[J]. Infrared and Laser Engineering, 2019, 48(6): 603010.

[5] PISAREV V, ODINTSEV I, ELEONSKY S, et al. Residual stress determination by optical interferometric measurements of hole diameter increments [J]. Optics and Lasers in Engineering, 2018, 110: 437-456.

[6] ZASLANSKY P, FRIESEM A A, WEINER S. Structure and mechanical properties of the soft zone separating bulk dentin and enamel in crowns of human teeth: Insight into tooth function [J]. Journal of Structural Biology, 2006, 153(2): 188-199.

[7] KUMAR M, SHAKHER C, AGARWAL R, et al. Deformation measurements in cortical bone-miniscrew interface in human maxilla by using digital speckle pattern interferometry [J]. Speckle 2018: VII International Conference on Speckle Metrology, 2018: 1083412.

[8] PAGLIARULO V, BIANCO V, MEMMOLO P, et al. Leaks detection in stainless steel kegs via ESPI [J]. Optics and Lasers in Engineering, 2018, 110: 220-227.

[9] GENOVESE K, LAMBERTI L, PAPPALETTERE C. A comprehensive ESPI based system for combined measurement of shape and deformation of electronic components [J]. Optics and Lasers in Engineering, 2004, 42: 543-562.

[10] KONG Ming, HAO Ling, LIU Wei, et al. Phase splicing algorithm based on optimized Harris corner in digital holography [J]. Infrared and Laser Engineering, 2019, 48(11): 1126002.

[11] YU Yingjie, CHEN Gang, DAI Cuixia, et al. Application of phase stitching technique on digital holography[J]. 2009, 38(11): 2975-2979.

[12] YAN Hao, ANAND A. Studies on aperture synthesis in digital Fresnel holography [J]. Optics and Lasers in Engineering, 2012, 50: 556-562.

[13] PELAGOTTI A, PATURZO M, LOCATELLI M, et al. An automatic method for assembling a large synthetic aperture digital hologram [J]. Optics Express, 2012, 20(5): 4830-4839.

[14] LIM S, CHOI K, HAHN J, et al. Image-based registration for synthetic aperture holography [J]. Optics Express, 2011, 19(12): 224-233.

[15] ZHANG Yu, LU Xiaoxu, LUO Yinlong, et al. Synthetic aperture holography by movement of object [J]. Holography, Diffractive Optics, and Applications II, 2005, 5636: 581-588.

[16] WEN Yongfu, QU Weijuan, CHENG Haobo, et al. Further investigation on the phase stitching and system errors in digital holography [J]. Applied Optics, 2015, 54(2): 266-276.

[17] CLAUS D. High resolution digital holographic synthetic aperture applied to deformation measurement and extended depth of field method [J]. Applied Optics, 2010, 49(16): 3187-3198.

[18] XU Xianfeng, LU Guangcan, HAN Guoxia, et al. Phase stitching and error correction in aperture synthesis for generalized phase-shifting interferometry [J]. Applied Optics, 2013, 52(20): 4864-4870.

[19] ARAI Y. Electronic speckle pattern interferometry based on spatial information using only two sheets of speckle patterns [J]. Journal of Modern Optics, 2014, 61(4): 297-306.

[20] QIAN Kemao. Two-dimensional windowed Fourier transform for fringe pattern analysis: principles, applications and implementations [J]. Optics and Lasers in Engineering, 2007, 45(2): 304-317.

[21] ZHAO Ming, QIAN Kemao. Quality-guided phase unwrapping implementation: an improved indexed interwoven linked list [J]. Applied Optics, 2014, 53(16): 3492-3500.

[22] PAN Bing, QIAN Kemao, XIE Huimin, et al. Two-dimensional digital image correlation for in-plane displacement and strain measurement: a review [J]. Measurement Science and Technology, 2009, 20(6): 1-17.

Phase Stitching Based Multi-CCDs Deformation Measurement in Digital Speckle Pattern Interferometry

LONG Jun[1,2], CAI Ping[1,2], PAN Shuyuan[1,2], LIU Chiyue[1,2], YAN Hao[1,2]
(1 *School of Electronic Information and Electrical Engineering, Shanghai Jiao Tong University, Shanghai* 200240, *China*)
(2 *Shanghai Engineering Research Center for Intelligent Diagnosis and Treatment Instrument, Shanghai* 200240, *China*)

Abstract: Digital Speckle Pattern Interferometry (DSPI) provides an effective means of full-field and non-contact measurement of deformation or displacement. With the advancement of the aerospace and automotive industry, deformation measurements with a large Field Of View (FOV), high resolution, and wide measurement range are becoming more and more urgent. However, it is difficult to increase the FOV for a given size of CCD without compromising the lateral resolution of the deformation measurement. To solve this problem, a technique for stitching the phases of multiple sub-images to enlarge the FOV without impairing the lateral resolution was investigated. The existing aperture synthesis methods usually obtained multi-images by moving CCD or object. They are only applicable to the measurement and observation of stationary objects. For deformation measurements, at least two surface states of the object are involved, corresponding to before and after deformation. Thus, the positioning errors and axial misalignment between corresponding hologram pairs are difficult to estimate. To overcome the disadvantages of multi-step image acquisition schemes. An experimental setup with multiple CCDs was constructed to obtain multiple sub-images. The phase of each CCD was extracted by the Fourier-transform method, and then the unwrapped phase maps of the overlapping areas were used to estimate the relative positions. Subsequently, the phase deviations between adjacent sub-image pairs were estimated and compensated for correct phase stitching. In order to obtain the largest possible FOV using as few CCDs as possible, the effect of the size of the overlap area on the stitching results was analyzed. The relationship between the standard deviation and the size of the overlapping area was investigated. The standard deviation is less than 0.015 μm when the size of the overlap area is between 141 and 461 pixels, corresponding to a percentage of the overlap area between 8.8% and 28.8%. Therefore, the size of the overlap area is approximately 10%, which may be appropriate in terms of the trade-off between FOV and accuracy. With the proposed method, the FOV was expanded from 5.5 cm×4 cm to 10 cm×4 cm and only two CCDs were used. The maximum relative error before and after stitching of the overlapping area was less than 1%, which illustrates the effectiveness of the proposed method. In addition, to further demonstrate the effectiveness of the phase stitching method, a calibrated loading device (the loading range is 0~9 μm, the expanded measurement uncertainty is 0.2 μm with the coverage factor k=2) is driven by a piezoelectric actuator was used. A total of 9 displacement loading points were included, and three groups of values were measured by CCD#1, CCD#2, and the phase stitching method. The Least-Square (LS) method was used to fit the measured deformation of the three groups and the fitting residuals were evaluated. Additionally, the coefficient of determination R and the Root Mean Square Error (RMSE) of the quality of the fitting were compared. The measurement accuracy of the phase stitching method was equivalent to that of the single-camera method when comparing the measurements of the calibration points by the Root Mean Square Error (RMSE) metric. In summary, the proposed phase stitching method based on multi-CCDs deformation measurement is an effective means to increase the FOV without impairing the lateral resolution. At the same time, with a certain FOV, the measurement range and axial resolution can increase. Theoretically, for the deformation distribution similar to the cantilever beam, the measurement range can increase with the increment of FOV.

Key words: Digital speckle pattern interferometry; Phase stitching; Phase errors; Deformation measurement; Multi-CCDs
OCIS Codes: 120.6165; 090.1995; 120.3180; 120.6160